ORIGINAL ARTICLE

RECORDS OF PHARMACEUTICAL AND BIOMEDICAL SCIENCES

# Anti-inflammatory Activity and HPTLC Phytochemical Screening of *Hibiscus sabdariffa* Leaves

***Nahla S. El-Gazzar*** [a,*], ***Doaa A. Ghareeb*** [b,c], ***Fatma A.A. Mahmoud*** [b], ***Ingy I. Abdallah*** [a]

[a] *Department of Pharmacognosy, Faculty of Pharmacy, Alexandria University, Egypt;* [b] *Bio-screening and Preclinical Trial Lab, Biochemistry Department, Faculty of Science, Alexandria University, Alexandria, Egypt;* [c] *Biochemistry Department, Faculty of Science, Alexandria University, Alexandria, Egypt*

**Received on: 01-10-2023**

**Revised on: 19-10-2023**

**Accepted on: 24-10-2023**

*Correspondence Author:

Phone: +201022624344

E-mail address:

shawky.nahla@yahoo.com,

nahla.elgazzar@alexu.edu.eg

## Abstract

*Hibiscus sabdariffa* L. is famous for its medicinal properties. The *in-vitro* anti-inflammatory activity of the total ethanolic extract and different fractions of *H. sabdariffa* leaves was evaluated. All samples demonstrated anti-inflammatory effect against the pro-inflammatory mediators, TNF-α, IL-1β, IFN-γ and IL-6, where the ethyl acetate fraction exhibited the highest activity. Additionally, untargeted and targeted metabolic profiling were performed using HPTLC-image analysis accompanied by multivariate analysis. This method has been implemented for the first time for the profiling of bioactive secondary metabolites in *H. sabdariffa* leaves correlated to its anti-inflammatory activity. Targeted metabolic profiling of the samples revealed the presence of lupeol, stigmasterol, β-sitosterol, ursolic acid, kaempferol, quercetin, stigmasterol glucoside, β-sitosterol glucoside, chlorogenic acid, rutin and kaempferol-3-O-glucoside, in addition to the tentative identification of a steryl glycoside and two flavonoids. Semi-quantitation of the identified compounds was established based on the peak areas of their corresponding spots on the TLC plates. Orthogonal projection to latent structures (OPLS) model correlated the HPTLC chromatographic data of the identified compounds with the anti-inflammatory activity revealing that kaempferol, quercetin, kaempferol-3-O-glucoside, flavonoid 1, flavonoid 2, rutin and chlorogenic acid are the chemical markers most contributing to the model. This is in line with their presence in high amount in the ethyl acetate fraction that displayed the greatest anti-inflammatory activity across all tested mediators. These results prove the potential of *H. sabdariffa* leaves as anti-inflammatory agent and the correlation of its content of flavonoids and phenolic acids to such activity.

**Keywords:** *Hibiscus sabdariffa*; anti-inflammatory; leaves; HPTLC, multivariate analysis

## 1. Introduction

Since ancient times plants have been an indispensable asset for humans as source of food and medicine. Genus *Hibiscus* belonging to family Malvaceae comprises approximately 300 species, of which several species are used as ornamental or culinary plants while numerous ones possess medicinal properties. *Hibiscus sabdariffa* L., commonly known as roselle, is a famous species that is easily cultivated in tropical and subtropical regions such as Egypt, Saudi Arabia, Sudan, India, Mexico, etc. It is well known for its medicinal properties and has been used in traditional folk medicine, in addition to its use in the food and

beverage industries. Stem, leaves, calyces and seeds of *H. sabdariffa* are all sought after parts for various applications. The different parts are rich in phytochemicals where calyces are characterized by high content of anthocyanins and flavonoids while phenolic acids and flavonoids are majorly present in the leaves. Whenever *Hibiscus* is mentioned, what comes to mind is the calyx of the plant and its use in teas and beverages with its distinctive red color and characteristic flavor. However, the leaves of *H. sabdariffa*, although less famous, are consumed raw or cooked in some countries and have been reported to possess several medicinal activities. Among these bioactivities are anti-oxidant, anti-cancer, anti-inflammatory, anti-atherosclerotic and anti-hyperlipidemic activities. It can also be used to improve digestive and kidney functions (Da-Costa-Rocha et al., 2014; Montalvo-González et al., 2022; Qi et al., 2016; Riaz et al., 2018; Singh et al., 2017). *H. sabdariffa* leaves collected from various regions under different cultivation conditions can show variation in their chemical composition which in turn may affect their medicinal effects (Lyu et al., 2020; Wang et al., 2015).

Inflammation is a normal physiological response of the body in response to injury or trauma. It is triggered by chemical mediators involving numerous cells and characterized by swelling, redness, warmth and pain. Although the complex series of events elicited by the inflammatory response aims at healing and repairing the damaged tissues, if left unchecked it can cause more harm than good. Several anti-inflammatory drugs are available in the market but they are usually accompanied by serious side effects such as gastric irritation, liver and kidney damage. Hence, there is a pressing need for safer effective alternative therapies. Herbal remedies represent such alternative and the leaves of *H. sabdariffa* constitute a promising candidate for anti-inflammatory evaluation (Apaza Ticona et al., 2022; Guddeti et al., 2015; Patil et al., 2017; Ramaevi et al., 2016; Zhen et al., 2016).

The aim of this study is the evaluation of the anti-inflammatory activity of the total ethanolic extract and different fractions of *H. sabdariffa* leaves collected in Egypt. In addition to, implementation of untargeted and targeted metabolic profiling of the extract and fractions using High-Performance Thin-Layer Chromatography (HPTLC)-image analysis accompanied by multivariate analysis to detect chemical markers correlated to the anti-inflammatory activity.

# 2. Experimental

## 2.1. Chemicals and reagents

Several reagents and chemicals employed in this research were procured from Sigma (St. Louis, Mo., USA) including RNA and cDNA extraction kits, RNase inhibitor, reverse transcriptase, nuclease free water, piroxicam, dimethyl sulfoxide (DMSO), lipopolysaccharides (LPS), trypan blue, SYBR green master mix, and MTT (3-(4,5-dimethylthiazol-2-yl)-2,5-diphenyl tetrazolium bromide) colors. Lonza (Belgium) supplied Roswell Park Memorial Institute (RPMI) 1640 Medium, fetal Bovine serum, and L-glutamine. Deoxynucleotide triphosphate (dNTPs) and dT primer were bought from Thermo Fisher Scientific.

Lupeol, stigmasterol, β-sitosterol, ursolic acid, β-sitosterol glucoside, stigmasterol glucoside, kaempferol, quercetin, kaempferol-3-O-glucoside, rutin and chlorogenic acid standards were purchased from Sigma-Aldrich (Darmstadt, Germany). Acetic acid, ethyl acetate, *n*-butanol, chloroform, methanol, ethanol and toluene were purchased from Merck (Darmstadt, Germany).

## 2.2. Plant collection, extraction and fractionation

Leaves of *H. sabdariffa* were collected from Kafr El-Sheikh, Egypt in April 2023. Prof. Dr. Salama El Dareer, Professor of Botany, Faculty of Science, Alexandria University, verified the plant's identity. H-SF-011 is a voucher specimen of *H. sabdariffa* leaves placed in the herbarium of the Department of Pharmacognosy, Faculty of Pharmacy, Alexandria University. The leaves (600 gm) were allowed to dry completely at ambient temperature. Air-dried leaves were crushed electrically into a coarse powder and macerated in 95% ethanol for 14 days in an air-tight, light-resistant container. Then, the hydro-ethanolic extract was collected and dried under vacuum using a rotatory evaporator (Buchi, rotavap210, Switzerland) at a temperature not exceeding 55°C and then weighed (the extraction yield was 280 gm). Moreover, the hydro-ethanolic extract was re-suspended in 50% ethanol and successively extracted with petroleum ether, chloroform, ethyl acetate and *n*-butanol in terms of increasing polarity. Finally, each fraction was filtered and concentrated to dryness under reduced pressure using a rotatory evaporator (Buchi, rotavap210, Switzerland) at a temperature not exceeding 55° C.

## 2.3. *In-vitro* cytotoxicity and anti-inflammatory activity testing of the total ethanolic extract and different fractions of *H. sabdariffa* leaves

MTT assay was carried out on isolated human white blood cells (WBCs) to evaluate the cytotoxicity of all *H. sabdariffa* samples expressed as EC100 and their

results were compared to that of standard piroxicam. Moreover, the effective anti-inflammatory concentration (EAIC) was estimated for each sample in lipopolysaccharide (LPS) stimulated human WBCs culture. The pro-inflammatory mediators TNF-α, IL-1β, IFN-γ and IL-6 expression levels were determined by real-time polymerase chain reaction. Fold change in gene expression was used to express the effect of LPS and *H. sabdariffa* samples on the pro-inflammatory genes expression. Results were expressed as means ± standard deviation (SD) of three individual replicates. For statistical analysis, one-way analysis of the variance (ANOVA) was applied using SPSS 26.0 program (SPSS Inc., Chicago, IL, USA) (Selim et al., 2023).

## 2.4. High Performance thin-layer chromatography accompanied by multivariate analysis

### *2.4.1. Preparation of plant samples*

50 mg of each of the dry residues of the total ethanolic extract and different fractions of *H. sabdariffa* leaves was weighed accurately and dissolved in 1 ml methanol followed by filtration using a syringe filter (0.2 µm) for subsequent application on HPTLC plates.

### *2.4.2. Reference standard solutions preparation*

Individual reference standards were precisely weighed and dissolved in methanol to a concentration of 0.5 mg/ml. STD MIX 1 was prepared by mixing the individual standard solutions of lupeol, stigmasterol, β-sitosterol, ursolic acid, stigmasterol glucoside and β-sitosterol glucoside while STD MIX 2 was composed of kaempferol and quercetin. Chlorogenic acid, rutin and kaempferol-3-O-glucoside constituted STD MIX 3.

### *2.4.3. High Performance thin-layer chromatography*

Samples and STD MIXs were spotted on (20 cm× 10 cm) silica gel HPTLC plates (Merck, Darmstadt, Germany) via CAMAG Linomat V automated spray-on band applicator (Muttenz, Switzerland) using a 100 µl syringe and controlled by WinCats manager software (Camag, 2008). Fourteen tracks; 12 lanes for plant samples and 2 lanes for STD MIXs; were applied per plate with 8 mm bandwidth, 5 mm inter-band spaces and 15 mm from the bottom and both margins of the plates. 10 µl of each of the total ethanolic extract, petroleum ether, chloroform and ethyl acetate fractions of *H. sabdariffa* leaves were applied in triplicate on chromatogram I accompanied by 8 µl of STD MIX 1 together with 5 µl of STD MIX 2. On the other hand, chromatogram II included 10 µl of each of the total ethanolic extract, chloroform, ethyl acetate and *n*-butanol fractions of *H. sabdariffa* leaves, in addition to 5 µl of STD MIX 3. Chromatogram I was developed in a mixture of toluene: ethyl acetate: methanol (9: 3: 1.25 v/v/v) while the mobile phase for developing chromatogram II was ethyl acetate: methanol: water: glacial acetic acid (27: 3: 1.5: 0.2 v/v/v/v). Twin-trough CAMAG glass chamber (10 x 20 cm) holding 50 ml mobile phase system was used for vertical development of the chromatograms for a distance of 95 mm. Both chromatograms were visualized under UV light at 254 nm and documented using a Samsung Galaxy triple lens camera (12 MP + 12 MP + 8 MP) then dipped in anisaldehyde/sulfuric acid reagent and heated at 120 ℃ followed by photographing in white light.

### *2.4.4. Image processing and multivariate data analysis for untargeted metabolic profiling*

The documented images were cropped, denoised and processed using Adobe Photoshop®. Then, ImageJ 1.51h (Wayne Rasband, NIH, USA) was utilized to generate line profile plots for each sample. The profile plots exhibit a 2D graph of the intensities of pixels along a fixed line. The data extracted from these profile plots was transferred to Microsoft Office Excel 2016 to calculate $R_f$ values accompanied by intensities for the image of each sample's track. The resulting data matrices represent HPTLC profiles of all samples. Multivariate processing of the HPTLC profiles was performed using SIMCA 14.1 software (Unmetrics AB, Umea, Sweden) where Principal Component Analysis (PCA) was engaged for untargeted metabolic profiling of the samples. Data preprocessing via multiplicative signal correction (MSC) and Savitzky-Golay filter were applied when needed. The models were evaluated for goodness of fitting and prediction ($R^2$ and $Q^2$). Loading line plots were generated to help in determination of significant chemical markers in the samples.

### *2.4.5. Image processing for targeted chemical analysis of the samples*

Sorbfil TLC Videodensitometer V 2.5 from (JSC Sorbpolymer) was utilized to compare $R_f$ values of the significant chemical markers determined from PCA loading line plots and those of reference standards in both chromatograms I and II, then spot peak areas of the identified compounds were estimated for semi-quantitation.

### *2.4.6. Orthogonal projection to latent structures (OPLS) model for targeted metabolic profiling*

The data matrix generated from the semi-quantitative analysis of compounds in the plant extract and fractions (X-matrix) along with the data matrix of the anti-inflammatory activities of the different samples (Y-matrix) were subjected to multivariate orthogonal projection to latent structures (OPLS) analysis using SIMCA 14.1 software (Umetrics, Umea, Sweden) for bio-profiling of the plant samples. This was attempted to determine the biomarkers correlated to the anti-

inflammatory activity. Coefficient plots were applied for identification of variables that can be considered positively or negatively correlated to the anti-inflammatory activity. In addition, a variable importance for the projection (VIP) plot was utilized to ascertain the compounds with significant contribution to the model; variables with VIP threshold more than 1 were considered essential. The model was evaluated for goodness of fitting and prediction ($R^2$ and $Q^2$). Additionally, Root Mean Squared Error of calibration (RMSEC) and Root Mean-Squared Error of Cross-Validation (RMSECV) were calculated.

# 3. Results and discussion

### 3.1. *In-vitro* cytotoxicity and anti-inflammatory activity of the total ethanolic extract and different fractions of *H. sabdariffa* leaves

The safety of the tested extracts and the anti-inflammatory standard (piroxicam) on normal White Blood Cells (WBCs) was assessed using 3-(4,5-dimethylthiazol-2-yl)-2,5-diphenyltetrazolium bromide (MTT) test and EC100 values that result in 100% cell viability were calculated (Fig. 1A). All the tested extracts showed EC100 values higher than that of the anti-inflammatory standard piroxicam (100 µg/ml) indicating their safety on WBCs and their anti-inflammatory activity can be assessed on Lipopolysaccharides (LPS)-stimulated WBCs. Our results evidenced that in the presence of up to 100 µg/mL of each extract, normal macrophages viability was not significantly lower than in non-treated cells as demonstrated in Fig. 1A. The survival rate of macrophage cells exposed to the total ethanolic extract, petroleum ether, chloroform, ethyl acetate and *n*-butanol fractions at the concentration of 100 µg/mL were all above 80%. Such results suggested that the studied extracts had no cytotoxicity on macrophages at a concentration up to 100 µg/ml. However, for piroxicam (100 µg/mL), the survival rate of macrophage cells was around 80%, indicating that the tested extracts were relatively safer than the reference drug on macrophages as presented in Fig. 1A. Furthermore, the effective anti-inflammatory concentrations (EAICs) (Fig. 1B) of the tested extracts and piroxicam that bring the excessive proliferation of LPS-stimulated WBCs to normal proliferation of non-stimulated cells (stimulation index = 1) were determined. The ethyl acetate (5.1681 µg/ml), petroleum ether (7.2241 µg/ml), chloroform (9.6891 µg/ml), *n*-butanol (14.1754 µg/ml) fractions exhibited much lower EAICs values compared to that of piroxicam (15.4333 µg/ml) indicating their great efficacy. However, the total ethanolic extract exhibited higher EAIC value (18.3997 µg/ml) compared to that of piroxicam. Moreover, the gene expression of four pro-inflammatory markers (TNF-α, IL-1β, IFN-γ, IL-6) by real time polymerase chain reaction (PCR) in normal WBCs and the treated WBCs with lipopolysaccharide was investigated. The results showed that the ethyl acetate, petroleum ether and chloroform fractions of *H. sabdariffa* reduced the 5.1-fold gene upregulation of TNF-α caused by LPS to levels of 0.51, 0.91 and 1.06-fold, respectively, lower than those produced by piroxicam (1.53-fold). On the other hand, the upregulation of IL-1β gene expression was reduced to 0.76, 1.37, 1.59 and 2.31-fold by the ethyl acetate, petroleum ether, chloroform fractions and the total ethanolic extract, respectively, compared to a 2.5-fold down regulation by piroxicam indicating their strong efficacy (Fig. 1C). In addition to that, when WBCs were treated with LPS, the expression of IFN-γ increased by 12.3 times, while treatment with the ethyl acetate, chloroform, *n*-butanol, petroleum ether fractions and the total ethanolic extract induced downregulation of gene expression by 0.30, 0.51, 0.62, 0.81 and 0.83-fold, respectively, in comparison to a 1.3-fold change after treatment with piroxicam. Furthermore, piroxicam lowered gene expression of IL-6 gene by 1.8-fold, while LPS increased IL-6 gene expression by 18.3-fold. The ethyl acetate, chloroform, *n*-butanol, petroleum ether fractions and the total ethanolic extract, all significantly reduced such elevated level of gene expression by 0.24, 0.41, 0.50, 0.65 and 0.66-fold, respectively, giving evidence that these fractions are more effective than piroxicam in reducing IL-6 gene expression (Fig. 1C). These findings demonstrated the anti-inflammatory effect of the tested extracts of *H. sabdariffa* against pro-inflammatory indicators such as TNF-α, IL-1β, IFN-γ, and IL-6. Several previous studies indicated the anti-inflammatory activity of genus *Hibiscus* (Apaza Ticona et al., 2022; Begum et al., 2018). These findings and our results revealed the importance of *H. sabdariffa* extracts as potential sources of anti-inflammatory constituents that can help in the treatment of various inflammatory conditions.

### 3.2. Untargeted metabolic profiling of the total ethanolic extract and different fractions of *H. sabdariffa* leaves using HPTLC-PCA analysis

HPTLC can be employed to discover the variation among different extracts qualitatively and quantitatively so it is recognized as a valued mean for targeted and untargeted metabolomics. Untargeted pattern recognition was used for the comparative metabolic profiling of the total ethanolic extract and fractions of *H. sabdariffa* leaves to explore sample distribution and discover possible patterns.

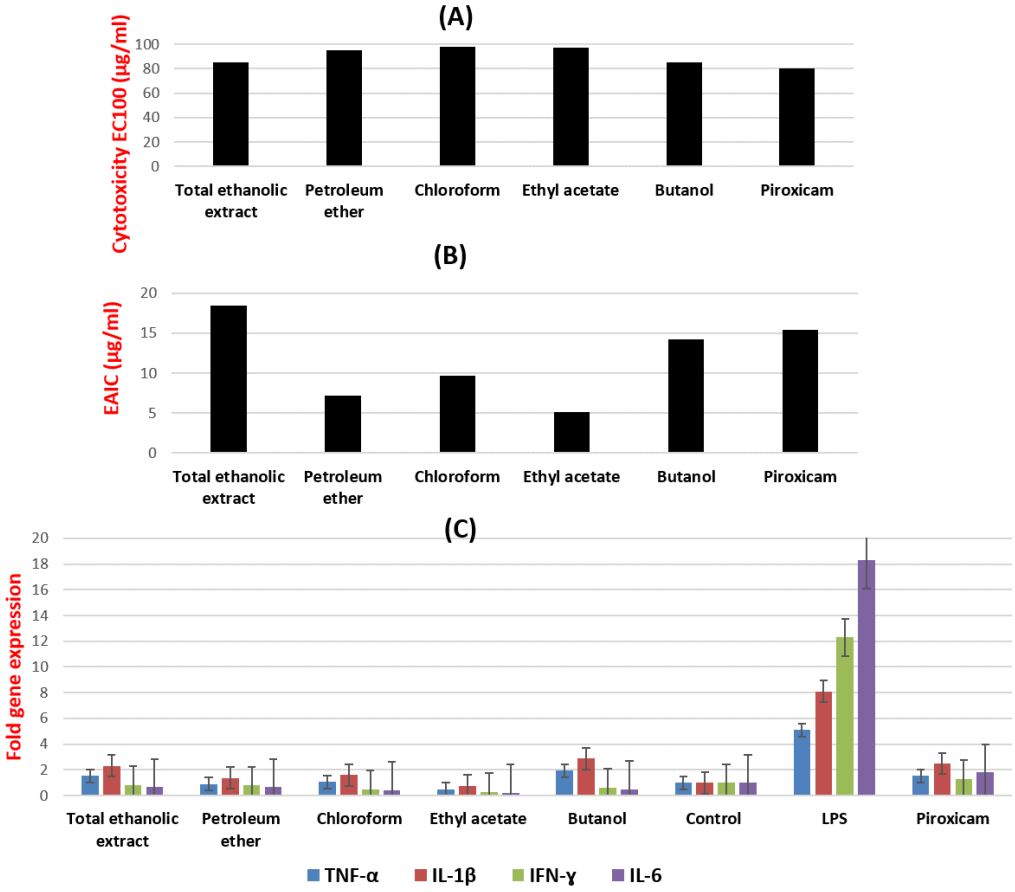


**Fig. 1. Bar charts showing (A) EC100, (B) Effective anti-inflammatory concentrations (EAICs) of tested extracts and (C) TNF-α, IL-1β, IFN-γ, IL-6 (expressed as fold change) of the tested samples**.

The HPTLC profile of chromatogram I (Fig. 2A), comprising total ethanolic extract, petroleum ether, chloroform and ethyl acetate fractions, recorded under white light following post-chromatographic derivatization with anisaldehyde/sulfuric acid revealed differences in the metabolic profile. The data matrix of digitized chromatogram I (36 samples X 1455 variables) was subjected to PCA. The resulting PCA score scatter plot (Fig. 2B) showed clear separation of the samples with total variance of 80.5%, where PC1 accounted for 65.7% and PC2 for 14.8%, at adjusted ellipse Hoteling of 95%. The total ethanolic extract samples were grouped at the negative side of both PC1 and PC2, on the contrary, the ethyl acetate fraction samples were grouped at the positive side of both. The petroleum ether fraction samples were clustered at the negative side of PC1 and positive side of PC2 while the chloroform fraction samples were grouped at the opposite side. The correlated loading plot (Fig. 2C) revealed that bands at $R_f$ 0.15, 0.23, 0.34, 0.36, 0.43, 0.52, 0.69, 0.74, 0.82, 0.87 and 0.97 had high contribution to the clustering pattern of the samples.

For profiling of compounds with higher polarity in the plant samples, chromatogram II (Fig. 2D) encompassing the total ethanolic extract, chloroform, ethyl acetate and butanol fractions of *H. sabdariffa* leaves was visualized and documented under UV light at 254 nm. Its digitalized data matrix (36 samples X 612 variables) generated PCA score scatter plot (Fig. 2E) that indicated 75.2% total variation among the samples with PC1 accounting for 55.9% and PC2 for 19.3% at adjusted ellipse Hoteling of 95%. The total ethanolic extract samples were grouped at the negative side of PC2 and on both sides of PC1 while the chloroform fraction samples were clustered at the negative side of PC1 and in between the positive and negative sides of PC2. On the other hand, the ethyl acetate samples were clearly separated on the negative side of PC1 and positive side of PC2 whereas butanol fraction samples were gathered at the positive side of both PC1 and PC2. Zones at Rf 0.11, 0.31, 0.45, 0.53, 0.65, 0.76 and 0.92, in the corresponding loading plot (Fig. 2F), had the highest impact on the PC1 and PC2 directions. The compounds with the highest contribution to PC1 and PC2 directions of the PCA plot of both chromatograms were targeted for further

identification and analysis. PCA of both chromatograms revealed clear separate clustering of the samples indicating the influence of the extraction solvent on metabolite distribution and abundance which in turn can affect the biological activity of the samples.

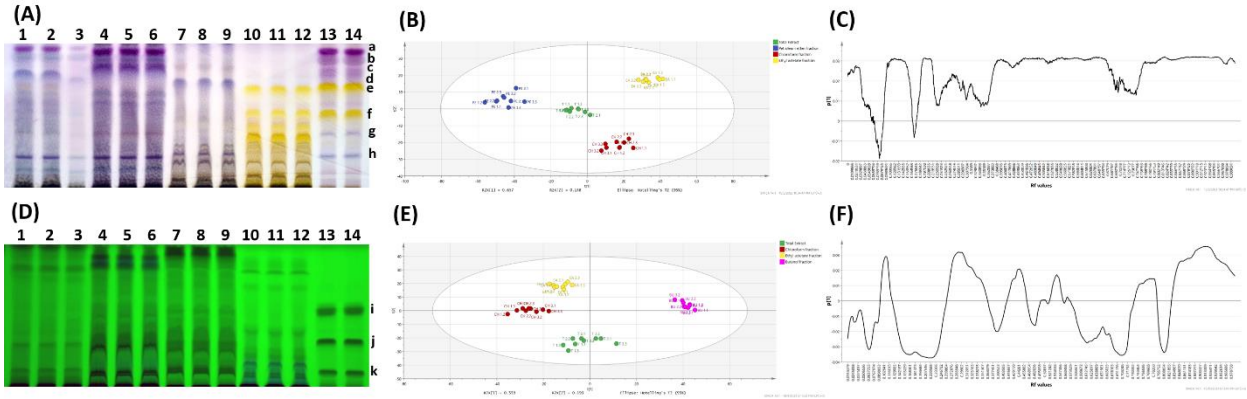


**Fig. 2. HPTLC-profiling of *H. sabdariffa* leaves. (A) Chromatogram I in white light after post-chromatographic derivatization with anisaldehyde/sulfuric acid reagent (Tracks 1-3; Total ethanolic extract, Tracks 4-6; Petroleum ether fraction, Tracks 7-9; Chloroform fraction, Tracks 10-12; Ethyl acetate fraction and Tracks 13&14; STD MIX 1 and 2, a: lupeol, b: stigmasterol, c: β-sitosterol, d: ursolic acid, e: kaempferol, f: quercetin, g: stigmasterol glucoside, h: β-sitosterol glucoside). (B) its PCA score scatter plot. (C) its corresponding loading plot. (D) Chromatogram II under UV at 254 nm (Tracks 1-3; Total ethanolic extract, Tracks 4-6; Chloroform fraction, Tracks 7-9; Ethyl acetate fraction, Tracks 10-12; Butanol fraction and Tracks 13&14; STD MIX 3, i: kaempferol-3-O-glucoside, j: rutin, k: chlorogenic acid). (E) its PCA score scatter plot. (F) its corresponding loading plot.**

### 3.3. HPTLC-targeted metabolic profiling of the total ethanolic extract and different fractions of *H. sabdariffa* leaves

Based on the results of the untargeted profiling, the $R_f$ values of the relevant bands in both chromatograms I and II were estimated and compared with $R_f$ of reference standard bands of STD MIXs (Fig. 2A and 2D) using Sorbfil TLC Videodensitometer V 2.5. In chromatogram I, the bands of $R_f$ values 0.23, 0.36, 0.52, 0.69, 0.74, 0.82, 0.87 and 0.97 were identified as lupeol, stigmasterol, β-sitosterol, ursolic acid, kaempferol, quercetin and stigmasterol glucoside, respectively. The band at $R_f$ 0.15 is suspected to be a steryl glycoside based on its migration on TLC and the color developed post derivatization with anisaldehyde/sulfuric acid while the bands at $R_f$ 0.34 and 0.43 were tentatively identified as flavonoids and denoted as flavonoid 1 and flavonoid 2, respectively. Zones of $R_f$ values 0.11, 0.31 and 0.53 in chromatogram II were recognized as chlorogenic acid, rutin and kaempferol-3-O-glucoside, respectively. The identified compounds are consistent with previous reports of the phytoconstituents of genus *Hibiscus* (Alam et al., 2018; dos Santos Nascimento et al., 2021; Lyu et al., 2020; Wang et al., 2015; Zhen et al., 2016). The peak areas corresponding to each of the identified spots on the HPTLC chromatograms were measured and utilized as an indication of the quantity of the compounds in the different samples.

### 3.4. OPLS modeling for discerning anti-inflammatory biomarkers

Orthogonal projection to latent structures (OPLS) was applied to ascertain which of the identified chemical constituents served as biomarkers that positively contributed to the anti-inflammatory activities of the various tested samples and to explore the clustering pattern of the samples based on their biological activities. An OPLS model to correlate the HPTLC chromatographic data and anti-inflammatory activities was created where the X matrix comprised the semi-quantitation results of the identified compounds (peak areas) while the Y matrix consisted of the data obtained from the anti-inflammatory activities (TNF-α, IL-1β, IFN-γ and IL-6). The performance of the constructed OPLS model was designated by the values of the coefficient of determination ($R^2$ 0.999) indicating the goodness of fitting, and the cross-validation redundancy ($Q^2$ 0.918) representing goodness of prediction.

The OPLS biplot (Fig. 3A) revealed that the ethyl acetate fraction samples displayed proximity to all the tested decreased pro-inflammatory mediators, where the flavonoids and phenolic acid were closely correlated to the tested biological activity. The biplot also revealed clear clustering of the ethyl acetate fraction samples isolated from the samples of the total extract, petroleum ether, chloroform and butanol

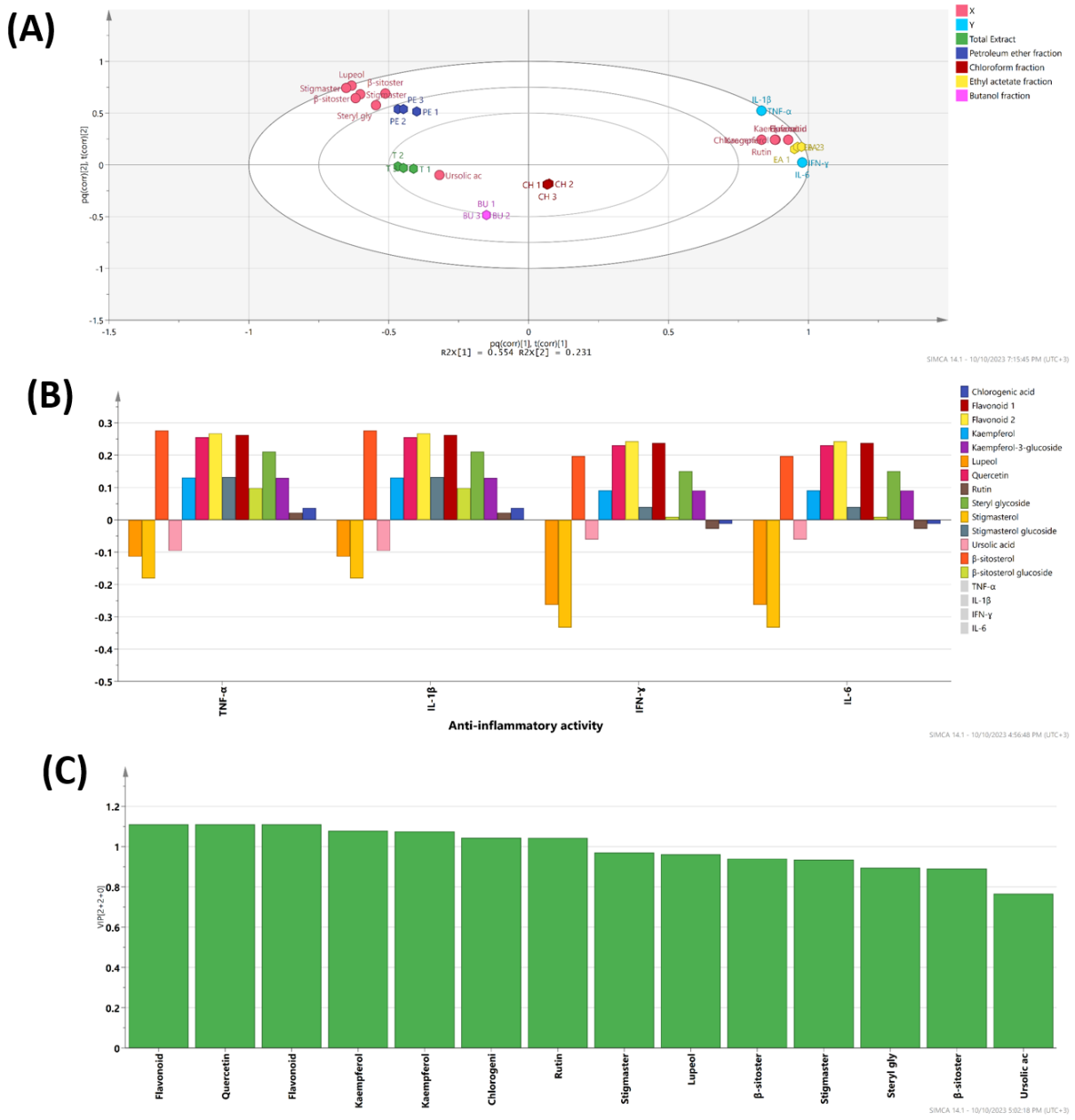


**Fig. 3. (A) OPLS biplot of total ethanolic extract and fractions of *H. sabdariffa* leaves, the identified chemical markers (X-variables) and the determined pro-inflammatory mediators, TNF-α, IL-1β, IFN-γ and IL-6 (Y-variables). (B) Correlation coefficient plot of each chemical marker to each pro-inflammatory mediator. (C) VIP plot of the OPLS model.**

fractions which are grouped separately but in closer proximity to each other. Furthermore, the correlation coefficient plot along with the variable importance in projection (VIP) plot were employed to detect the biomarkers in the samples. The correlation coefficient plot (Fig. 3B) representing the strength of associations between the X-variables and the Y-variables revealed that kaempferol, quercetin, kaempferol-3-O-glucoside, flavonoid 1 and flavonoid 2 are major positive contributors to the anti-inflammatory activity across all tested pro-inflammatory mediators. Rutin and chlorogenic acid showed minimal positive contribution against tested TNF-α and IL-1β while stigmasterol glucoside, β-sitosterol glucoside and steryl glycoside exhibited some positive contribution. In addition, chemical markers having the highest impact on the OPLS model could be determined from the VIP plot (Fig. 3C). The most noteworthy chemical

markers for the model were yet again kaempferol, quercetin, kaempferol-3-O-glucoside, flavonoid 1, flavonoid 2, rutin and chlorogenic acid (variables with VIP values above 1), endorsing the earlier results. These results are consistent with the fact that the ethyl acetate fraction exhibited the highest anti-inflammatory activity across all tested mediators which is suggested to be correlated to its high content of flavonoids and phenolic acids.

## 4. Conclusion

The potential of *H. sabdariffa* leaves as an anti-inflammatory was proven through the significant effect of its total ethanolic extract and fractions on the pro-inflammatory mediators (TNF-α, IL-1β, IFN-γ, IL-6) with the ethyl acetate fraction exhibiting the highest anti-inflammatory effect. Untargeted and targeted HPTLC fingerprinting were successfully achieved for rapid comparative fingerprint profiling of secondary metabolites, including sterols, flavonoids and phenolic acids in the total ethanolic extract and different fractions of *H. sabdariffa* leaves with the aim of unraveling the chemical and biological profiles of the different samples. Based on the metabolic profiling, lupeol, stigmasterol, β-sitosterol, ursolic acid, kaempferol, quercetin, stigmasterol glucoside, β-sitosterol glucoside, chlorogenic acid, rutin and kaempferol-3-O-glucoside were identified in the different *H. sabdariffa* samples, in addition to the tentative identification of a steryl glycoside and two flavonoids. The identified compounds were responsible for the clear clustering of the samples correlated to the extraction solvent used. The OPLS model allowed the determination of the most significant biomarkers correlated to the anti-inflammatory activity revealing that flavonoids and phenolic constituents have higher contribution to the activity compared to sterols. These findings encourage further investigation of *H. sabdariffa* and its phytoconstituents for its application as an anti-inflammatory agent.

## 5. References

Alam, P., Al-Yousef, H. M., Siddiqui, N. A., Alhowiriny, T. A., Alqasoumi, S. I., Amina, M., Hassan, W. H. B., Abdelaziz, S., & Abdalla, R. H. (2018). Anticancer activity and concurrent analysis of ursolic acid, β-sitosterol and lupeol in three different Hibiscus species (aerial parts) by validated HPTLC method. *Saudi Pharmaceutical Journal*, *26*(7), 1060–1067. doi: https://doi.org/10.1016/j.jsps.2018.05.015

Apaza Ticona, L., Pérez-Uz, B., García Esteban, M. T., Aguilar Rico, F., & Slowing, K. (2022). Anti-melanogenic and Anti-inflammatory Activities of Hibiscus sabdariffa. *Revista Brasileira de Farmacognosia*, *32*(1), 127–132. doi: 10.1007/s43450-022-00236-y

Begum, Z., Younus, I., & Khan, H. (2018). Analgesic and anti-inflammatory activities of the ethanol extract of Hibiscus rosa sinensis Linn (roots). *Pakistan Journal of Pharmaceutical Sciences*, *31*(5), 1927–1933.

Da-Costa-Rocha, I., Bonnlaender, B., Sievers, H., Pischel, I., & Heinrich, M. (2014). Hibiscus sabdariffa L. – A phytochemical and pharmacological review. *Food Chemistry*, *165*, 424–443. doi: https://doi.org/10.1016/j.foodchem.2014.05.002

dos Santos Nascimento, L. B., Gori, A., Raffaelli, A., Ferrini, F., & Brunetti, C. (2021). Phenolic Compounds from Leaves and Flowers of Hibiscus roseus: Potential Skin Cosmetic Applications of an Under-Investigated Species. In Plants (Vol. 10, Issue 3). doi: 10.3390/plants10030522

Guddeti, V., Madhu Babu, D., Nagamani, B., Ratna Teja, M., Sravani, M. S., & Spandana, C. (2015). EVALUATION OF ANTI INFLAMMATORY ACTIVITY OF HIBISCUS ROSA SINENSIS Linn. FLOWER EXTRACT IN RATS. *Ijpcbs 2015*, *5*(3), 532–536.

Lyu, J. Il, Kim, J. M., Kim, D.-G., Kim, J.-B., Kim, S. H., Ahn, J.-W., Kang, S., Ryu, J., & Kwon, S.-J. (2020). Phenolic Compound Content of Leaf Extracts from Different Roselle (Hibiscus sabdariffa) Accessions. *Plant Breeding and Biotechnology*. Retrieved from https://api.semanticscholar.org/CorpusID:216261771

Montalvo-González, E., Villagrán, Z., González-Torres, S., Iñiguez-Muñoz, L. E., Isiordia-Espinoza, M. A., Ruvalcaba-Gómez, J. M., Arteaga-Garibay, R. I., Acosta, J. L., González-Silva, N., & Anaya-Esparza, L. M. (2022). Physiological Effects and Human Health Benefits of Hibiscus sabdariffa: A Review of Clinical Trials. In Pharmaceuticals (Vol. 15, Issue 4). doi: 10.3390/ph15040464

Patil, S. B., & Munoli, S. (2017). Evaluation of anti - inflammatory activity of aqueous extract of leaves of hibiscus sabdariffa in albino rats. *International Journal of Basic & Clinical Pharmacology*, *6*(5), 1155. doi: 10.18203/2319-2003.ijbcp20171669

Qi, Y., Chin, K. L., Malekian, F., Berhane, M., &

Gager, J. (2016). Biological Characteristics, Nutritional and Medicinal Value of Roselle, Hibiscus Sabdariffa Biological Characteristics, Nutritional and Medicinal Value of Roselle, Hibiscus Sabdariffa. *Agricultural Research and Extension Center*, *70813*(MARCH 2005), 603–604.

Ramaevi, D., Rao, B. G., & Rajeshwari, V. (2016). Anti-Inflammatory Activity on Hibiscus sabdariffa Seeds. *International Journal of Current Microbiology and Applied Sciences*, *5*(7), 537–541. doi: 10.20546/ijcmas.2016.507.058

Riaz, G., & Chopra, R. (2018). A review on phytochemistry and therapeutic uses of Hibiscus sabdariffa L. *Biomedicine & Pharmacotherapy*, *102*, 575–586. doi: https://doi.org/10.1016/j.biopha.2018.03.023

Selim, D. A., Shawky, E., Ghareeb, D. A., Abdulmalek, S. A., & Abu El-Khair, R. M. (2023). Comparative metabolomics of the different fractions of two saltwort (Salsola L.) species in relation to their anti-inflammatory activity. *Food Bioscience*, *51*, 102306. doi: https://doi.org/10.1016/j.fbio.2022.102306

Singh, P., Khan, M., & Hailemariam, H. (2017). Nutritional and Health Importance of Hibiscus Sabdariffa: A Review and Indication for Research Needs. *Journal of Nutritional Health & Food Engineering*, *6*(5), 125–128. doi: 10.15406/jnhfe.2017.06.00212

Wang, J., Cao, X., Qi, Y., Ferchaud, V., Chin, K. L., & Tang, F. (2015). High-Performance Thin-Layer Chromatographic Method for Screening Antioxidant Compounds and Discrimination of Hibiscus sabdariffa L. by Principal Component Analysis. *JPC – Journal of Planar Chromatography – Modern TLC*, *28*(4), 274–279. doi: 10.1556/1006.2015.28.4.2

Zhen, J., Villani, T. S., Guo, Y., Qi, Y., Chin, K., Pan, M.-H., Ho, C.-T., Simon, J. E., & Wu, Q. (2016). Phytochemistry, antioxidant capacity, total phenolic content and anti-inflammatory activity of Hibiscus sabdariffa leaves. *Food Chemistry*, *190*, 673–680. doi: https://doi.org/10.1016/j.foodchem.2015.06.006